Appl. Phys. B 76, 583–586 (2003)
DOI: 10.1007/s00340-003-1132-8

Applied Physics B
Lasers and Optics

S.A. HOSSEINI✉
B. FERLAND
S.L. CHIN

Measurement of filament length generated by an intense femtosecond laser pulse using electromagnetic radiation detection

Centre d'Optique, Photonique et Laser, Université Laval, Québec G1K 7P4, Canada

Received: 6 November 2002/Revised version: 27 January 2003
Published online: 24 April 2003 •

ABSTRACT We present a new method to measure the length of a filament induced by the propagation of intense femtosecond laser pulses in air. We used an antenna to detect electromagnetic pulses radiated from multipole moments inside the filament oscillating at the plasma frequency. The results are compared with the values detected from the backscattered fluorescence induced by multiphoton ionization of nitrogen molecules excited inside the filament. The values are found to be in good agreement.

PACS 42.65.Jx; 42.68.Ay; 42.68.Wt

1 Introduction

Remote sensing, lidar (light detection and ranging) [1–3] and lightning discharge control [4–8] are potential applications of propagation of intense femtosecond laser pulses in air. Experimental results in the laboratory have shown that such pulses can propagate tens of meters in air and up to several kilometers in the atmosphere, beyond the Rayleigh range of the laser beam [9–19]. There are several models to explain the phenomenon, including self-guided pulse propagation [9–13], the moving focus model [14–17] and dynamic spatial replenishment [18]. When an intense femtosecond laser pulse propagates in air, the air acts as a Kerr nonlinear medium and focuses the beam (self-focusing). In the focusing region, the peak intensity increases and multiphoton ionization (MPI) is induced, resulting in plasma generation. The dynamical balance between the self-focusing and defocusing by the plasma yields a narrow ($\sim 100\,\mu$m diameter) and long plasma column (filament) up to tens of meters or more. The balancing act results in a maximum peak intensity, which we call intensity clamping. In air, it is about $5 \times 10^{13}\,\mathrm{W/cm^2}$ [19–21]. (In fact, R. Sauerbrey from Jena, Germany was the first to predict this balancing act resulting in a maximum intensity. Private communication, unpublished, March 1993.)

Having accurate knowledge of the length of a filament is essential in lightning control and remote sensing. Since the intensity inside the self-focusing laser pulse is very high, incorporating measurement devices directly into the beam is very difficult and it would damage the optical instruments. In this work we examine different methods to indirectly measure the length of a filament.

The plasma produced inside the filament contains free electrons and ions that are displaced from each other along the propagation direction [22]. This results in a multipole oscillation yielding radiation. This radiation was detected by a linear antenna for a single filament [22]. A simple theoretical model has been made for the dipole radiation [23]. In this work, we tested a new detector, a wire antenna, to detect this radiation. We call this the electromagnetic pulse (EMP) detection technique.

Other known techniques are measuring the conductivity of the filament [2, 24] and backscattering fluorescence (BSF) measurement [25]. In this work we compare the EMP and BSF techniques. We found that the EMP radiation measurement is a fast and more precise method for measuring the length of a filament as compared to the BSF method. However, the EMP detection method is not practical for very long horizontal propagation measurements and impossible for vertical propagation, while the BSF method could be applied to both situations.

2 Experimental setup and results

The versatile multibeam laser system used in this experiment was built by Spectra-Physics (SP)/Positive Light. It is a chirped pulse amplification system based on a Ti:sapphire oscillator (SP, Maitai, 300 mW, 80 MHz), a stretcher, a regenerative amplifier (SP, Spitfire, 2 W, 1 kHz), a two-pass Ti:sapphire amplifier and a pulse slicer (Pockels cell). A beam with a repetition rate of 10 Hz is extracted from the 1 kHz beam using the slicer. This beam is sent to a two-pass Ti:sapphire amplifier, pumped by the second harmonic of a Nd:YAG laser (SP, GCR-350, 500 mJ/pulse, 10 Hz). Finally the pulse is compressed to 44 fs (FWHM). The pulse duration is measured using a single-shot auto-correlator (Positive Light SSA). The central wavelength is 810 nm with a bandwidth of 23 nm (FWHM) and a peak power of 0.2 TW with linear polarization. The pulse is spatially filtered after the regenerative amplifier and before the two-pass amplifier in order to keep a near-Gaussian pulse shape. The pulse energy is fixed at 14 mJ.

✉ Fax: +1-418/656-2623, E-mail: shosseini@phy.ulaval.ca

In the first step, the experimental setup is designed to measure BSF as shown in Fig. 1. The laser beam is focused by a spherical concave gold mirror (CM) with a focal length of 3.5 m, since without a focusing mirror the filament length is beyond the dimension of our laboratory. The angle between the incident beam and the reflected beam is 4 degrees. This angle is minimized to minimize geometrical aberration. The filament starts to develop before the geometrical focus of the mirror and it is weakly visible by the naked eye. The BSF is detected by a photomultiplier tube (PMT) (Hamamatsu R74000U, with 1 ns resolution). A broadband dielectric mirror (M2) reflecting at around 800 ± 25 nm is put in front of the PMT to eliminate any scattering of the laser light. Also, a band-pass filter F (UG 11, 5 mm thick, passing 200 to 400 nm) is set between the PMT and the 800 nm dielectric mirror. This band-pass filter transmits only the UV region, where the major spectral lines are radiated from nitrogen molecules during the ionization [26]. The PMT is connected to a 1 GHz bandwidth oscilloscope (Tektronix TDS 7254, 2.5 GHz sampling rate) having a 50 Ω input impedance. Since the production of plasma inside the filament is a statistical phenomenon and heavily related to the fluctuations of the laser energy and air turbulence, we accumulate the waveforms coming from the oscilloscope for 2000 shots. After averaging about 500 shots there was no significant change in the final result but, to get a more precise result, we averaged the waveform for 2000 shots. Figure 2 shows a typical result. The first peak is due to scattering from the last mirror (M3) in the setup. The middle curve is the BSF signal from the filament. After the geometrical focus we observe a third peak, which is the result of refocusing [26]. In Fig. 2, we consider the geometrical correction factor $1/r^2$, where r is the distance between the PMT and the detected part of the filament, to compensate for the decrease of the BSF signal. This factor gives us the possibility to compare signals from different positions of the filament. One filament is observed with a total length of about 135 ± 15 cm. This value is arbitrarily defined between the 10% level of the maximum amplitude of the BSF signal [25] (see Fig. 2). We neglect the refocusing part since it is weaker than 10% of the maximum amplitude according to our definition. Since the resolution of the PMT is 1 ns (30 cm), it can not resolve the BSF signal (radiated from the beginning of the filament) and the scattered light from the last mirror of the setup. For this reason the two signals are mixed and it is impossible to determine precisely the starting point of the filament. We made an extrapolation of the signal by adding a tail (dotted curve) in Fig. 2 to indicate roughly the starting of the fluorescence signal.

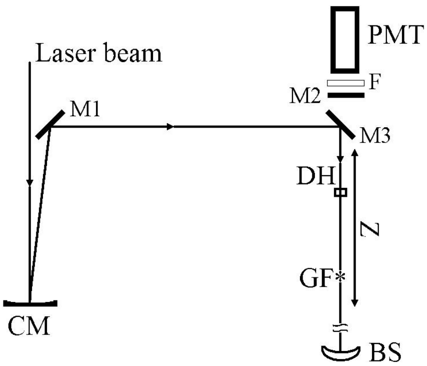

FIGURE 1 Schematic diagram of experimental setup. M1, M2, M3, dielectric mirrors; CM, concave gold mirror with focal length of 3.5 m; F, UG11 filter; DH, detector holder; GF, geometrical focus; BS, beam stop

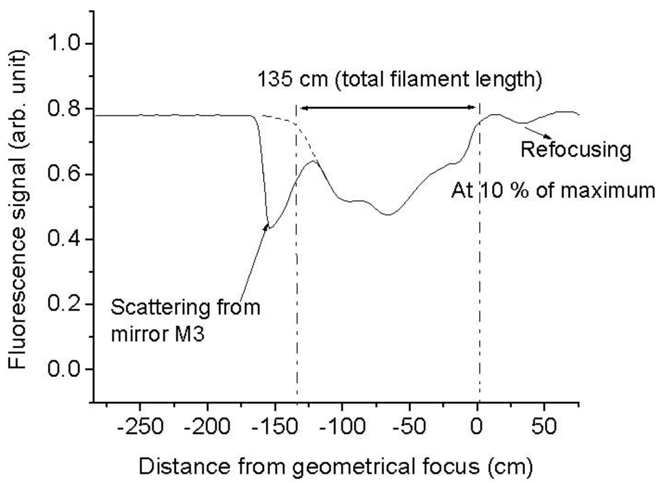

FIGURE 2 BSF signal collected by oscilloscope. The first peak is due to scattering from the last mirror (M3) in the setup and the last peak is due to refocusing

For the next step we put a 2 m long rail parallel to the laser beam. We placed a linear antenna on that rail, 5 mm away from the filament and perpendicular to the optical table as shown in Fig. 3a. The antenna is the inner core of a 50 Ω coaxial cable with 15 mm length. One of the waveforms detected by this antenna is shown in Fig. 4a. Each pixel represents 50 ps, which is the limit of our oscilloscope. This signal is caused by the electric field radiated from the plasma column [22, 23]. The antenna was moved by intervals of 2 cm over almost 200 cm. The amplitude of the signal detected by the antenna is plotted as a function of distance in Fig. 4b. We can see changes in the plasma density by changing the distance of the antenna from the geometrical focus. Higher amplitude signals represent higher plasma production inside the filament. The two major humps represent refocusing. The small oscillations in the graph are caused by the dynamics of multipole moments produced along the propagation direction. Since the formation of filaments is a statistical process and depends on laser pulse energy fluctuations, air turbulence, etc., the amplitude of these small oscillations can change in time; therefore we made an average of the signal over 20 shots. This data is reproducible, meaning that those small oscillations will be at the same position if we keep the same conditions. (We are now conducting more investigations to understand this phenomenon more precisely.) Since the filament is long and the

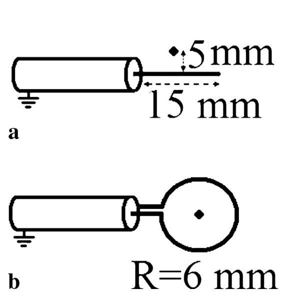

FIGURE 3 **a** Linear antenna and **b** circular antenna; these two antennas are moved along the z direction with a step of 2 cm (the *small dot* is the profile of the filament)

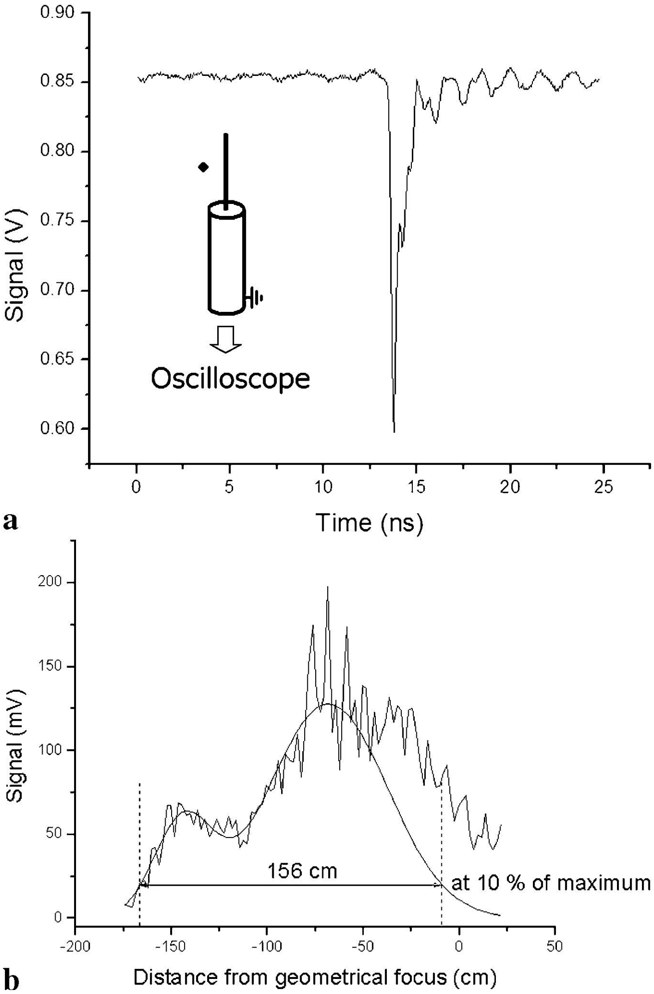

FIGURE 4 **a** Sample signal collected with the linear antenna. The signal is averaged over 20 shots. **b** Amplitude of the first peak collected with the linear antenna at different positions with respect to the geometrical focus of the concave gold mirror

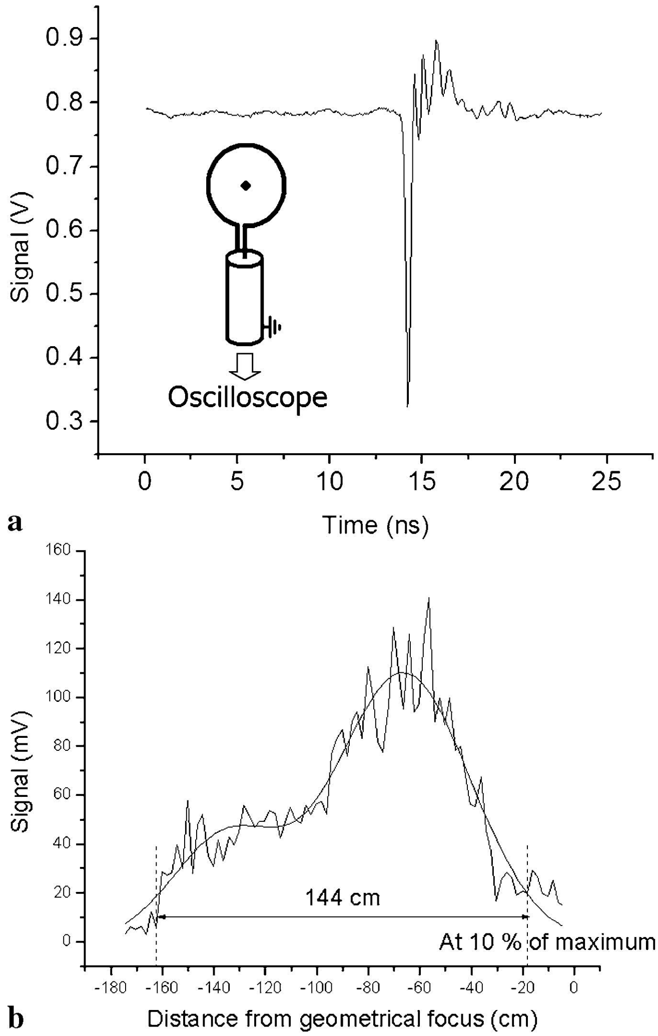

FIGURE 5 **a** Sample signal collected with the circular antenna. The signal is averaged over 20 shots. **b** Amplitude of the first peak collected with the circular antenna at different positions with respect to the geometrical focus of the concave gold mirror

conical emission [16] starts to take place before the geometrical focus, the beam diameter starts to increase and a part of the beam hits the detector (antenna) at about 45 cm before the geometrical focus. In this region the intensity of the beam is strong enough to induce a plasma on the antenna surface, causing an increase of the electrical signal. Therefore, the signal level will not fall as rapidly as it should and it does not reach its minimum. In this situation the weak refocusing signal after the geometrical focus is masked. If we put the detector too far from the filament we can no longer collect the signal. Nevertheless, it suggests a filament length of 156 cm neglecting all the data after point −45 cm. This value is arbitrarily defined between the 10% level of the maximum amplitude of the double-Gaussian graph fitted to the data. This is a major problem of using a linear antenna for measuring a very long filament length.

To try to solve this problem we designed another similar detector (circular antenna) by circling the linear antenna and connecting it to the outer core of the coaxial cable. It has 12 mm diameter and the filament passes through the center of it, as shown in Fig. 3b. A typical waveform detected by this detector is shown in Fig. 5a. Again we measured the peak (minimum) amplitude with respect to the distance from the geometrical focus of the concave mirror. The result is shown in Fig. 5b. Its general form is similar to that obtained by the linear antenna. It suggests a length of about 144 cm for the whole filament, neglecting refocusing after the geometrical focus. Again this value is measured between the 10% level of the maximum amplitude of the double-Gaussian graph fitted to the data. This is in agreement with the length measured with the BSF technique.

3 Conclusion

We have measured the length of a filament created by the propagation of intense femtosecond laser pulses in air. We show that the lengths of the filament determined by EMP detection and BSF measurement are in good agreement. With EMP detection we can see the dynamics of plasma production; higher amplitude signals are proportional to higher plasma production inside the filament. We can not observe these dynamics with BSF measurement because of the 1-ns resolution of the PMT detector. BSF measurement is good for measuring very long distance propagation in the atmosphere, whereas this can not be done with the EMP detection method.

ACKNOWLEDGEMENTS We wish to thank Dr. P. Agostini, Dr. A. Iwasaki and Dr. G. Roy for helpful discussions. We also acknowledge the technical expert assistance of M. Martin. This work is supported in part by NSERC, CIPI, DRDC-Valcartier, CFI, FQRNT, Canada Research Chair and NATO.

REFERENCES

1 L. Wöste, C. Wedekind, H. Wille, P. Rairoux, B. Stein, S. Nikolov, C. Werner, S. Niedermeier, F. Ronneberger, H. Schillinger, R. Sauerbrey: Laser Optoelektron. **29**, 51 (1997)
2 H. Schillinger, R. Sauerbrey: Appl. Phys. B: Lasers Opt. **68**, 753 (1999)
3 P. Rairoux, H. Schillinger, S. Niedermeier, M. Rodriguez, F. Ronneberger, R. Sauerbrey, B. Stein, D. Waite, C. Wedekind, H. Wille, L. Wöste, C. Ziener: Appl. Phys. B **71**, 573 (2000)
4 X.M. Zhao, J.-C. Diels, C.V. Wang, J.M. Elizondo: IEEE J. Quantum Electron. **QE-31**, 599 (1995)
5 X.M. Zhao, S. Diddams, J.-C. Diels: In *Tunable Laser Applications*, ed. by F.J. Duarte (Marcel Dekker, New York 1995) p. 113
6 S. Tzortzakis, B. Prade, M. Franco, A. Mysyrowicz, S. Hüller, P. Mora: Phys. Rev. E **64,** 57401 (2001)
7 H. Pépin, D. Comtois, F. Vidal, C.Y. Chien, A. Desparois, T.W. Johnston, J.C. Kieffer, B. La Fontaine, F. Martin, F.A.M. Rizk, C. Potvin, P. Couture, H.P. Mercure, A. Bondiou-Clergerie, P. Lalande, I. Gallimberti: Phys. Plasmas **8**, 2532 (2001)
8 M. Rodriguez, R. Sauerbrey, H. Wille, L. Wöste, T. Fujii, Y.-B. Andr, A. Mysyrowicz, L. Klingbeil, K. Rethmeier, W. Kalkner, J. Kasparian, E. Salmon, J. Yu, J.-P. Wolf: Opt. Lett. **27**, 772 (2002)
9 A. Braun, G. Korn, X. Liu, D. Du, J. Squier, G. Mourou: Opt. Lett. **20**, 73 (1995)
10 E.T.J. Nibbering, P.F. Curley, G. Grillon, B.S. Prade, M.A. Franco, F. Salin, A. Mysyrowicz: Opt. Lett. **21**, 62 (1996)
11 P.F. Curley, E.T.J. Nibbering, G. Grillon, R. Lange, M.A. Franco, T. Lehner, B. Prade, A. Mysyrowicz: In *Ultrafast Phenomena X*, Vol. 62, ed. by P.F. Barbara, J.G. Fujimato, W.H. Knox, W. Zinth (Springer, Berlin 1996) p. 103
12 H.R. Lange, G. Grillon, J.F. Ripoche, M.A. Franco, B. Lamouroux, B.S. Prade, A. Mysyrowicz: Opt. Lett. **23**, 120 (1998)
13 S. Tzortzakis, M.A. Franco, Y.-B. André, A. Chiron, B. Lamouroux, B.S. Prade, A. Mysyrowicz: Phys. Rev. E **60**, R3505 (1999)
14 A. Brodeur, C.Y. Chien, F.A. Ilkov, O.G. Koserava, V.P. Kandidov: Opt. Lett. **22**, 304 (1997)
15 O.G. Kosereva, V.P. Kandidov, A. Brodeur, S.L. Chin: J. Nonlinear Opt. Phys. Mater. **6**, 485 (1997)
16 S.L. Chin, A. Brodeur, S. Petit, O.G. Kosareva, V.P. Kandidov: J. Nonlinear Opt. Phys. Mater. **8**, 121 (1999)
17 N. Aközbek, C.M. Bowden, A. Talebpour, S.L. Chin: Phys. Rev. E **61**, 4540 (2000)
18 M. Mlejnek, E.M. Wright, J.V. Moloney: Opt. Lett. **23**, 382 (1998); M. Mlejnek, M. Kolesik, J.V. Moleney, E.M. Wright: Phys. Rev. Lett. **83**, 2938 (1999)
19 J. Kasparian, R. Sauerbrey, S.L. Chin: Appl. Phys. B **71**, 877 (2000)
20 A. Becker, N. Akozbek, K. Vijayalakshmi, E. Oral, C.M. Bowden, S.L. Chin: Appl. Phys. B **73**, 287 (2001)
21 W. Liu, S. Petit, A. Becker, N. Akozbek, C.M. Bowden, S.L. Chin: Opt. Commun. **202**, 189 (2002)
22 A. Proulx, A. Talebpour, S. Petit, S.L. Chin: Opt. Commun. **174**, 305 (2000)
23 C.-C. Cheng, E.M. Wright, J.V. Moloney: Phys. Rev. Lett. **87**, 213001 (2001)
24 S. Tzortzakis, B. Prade, M. Franco, A. Mysyrowicz: Opt. Commun. **181**, 123 (2000)
25 A. Iwasaki, N. Akozbek, B. Ferland, Q. Luo, G. Roy, C.M. Bowden, S.L. Chin: Appl. Phys. B, DOI 10.1007/s00340-002-1077-3
26 A. Talebpour, S. Petit, S.L. Chin: Opt. Commun. **171**, 285 (1999)